the pre-hydrogen-bonded anion radical is twice as much as that for the anion radical hydrogen-bonded by one molecule.

Conclusion

The electron spin-echo and the optical spectroscopic studies of benzophenone anion radical in the glassy matrix of ethanol and ethanol/MTHF showed that the spectral shift is caused by the formation of hydrogen bonding with one or two alcohol molecules located above and below the molecular plane of the anion radicals. The alcohol molecules hydrogen-bonded to the neutral benzophenone do not induce the spectral shift because the nonbonding orbital used for the formation of the hydrogen bonding is orthogonalized to the π^* and π^{**} orbitals responsible to the optical transition. Aromatic ketones show large spectral shifts in protic solvents because they form hydrogen bonding with the solvents through the p_z orbital on the ketone oxygen.

Registry No. Benzophenone radical anion, 16592-08-8; ethanol, 64-17-5; 2-methyltetrahydrofuran, 96-47-9.

Dielectric Relaxation Studies on Analogues of the Polypentapeptide of Elastin

René Buchet, Chi-Hao Luan, Kari U. Prasad, R. Dean Harris, and Dan W. Urry*

Laboratory of Molecular Biophysics, The University of Alabama at Birmingham, University Station/P.O. Box 311, Birmingham, Alabama 35294 *(Received: May 5, 1987; In Final Form: July 22, 1987)*

Dielectric measurements of the complex permittivity of coacervate concentrations of two analogues of the polypentapeptide of elastin, $(Xxx^1\text{-}Pro^2\text{-}Gly^3\text{-}Val^4\text{-}Gly^5)_n$ where Xxx is Val for the elastin polypentapeptide and Ile and Leu for the two analogues, were taken over the frequency range 1–1000 MHz and over the temperature range 0–60 °C. Two relaxation processes were observed in each polypentapeptide. One relaxation has a frequency centered in the low megahertz frequency range, which has been attributed to a low-frequency librational mode within the polypeptide. The other relaxation is located near the gigahertz frequency range. The magnitude of the dielectric increment, $\Delta\epsilon$, of the librational mode of each polypentapeptide analogue increases with increasing temperature from near zero at 0 °C to approximately 40 at 60 °C, showing an inverse temperature transition to a more ordered structure. Conversely, the magnitudes of the dielectric increment of the high-frequency relaxation decrease with increasing temperature and differ in approximate proportion to the hydrophobicity of the pentamer for the polypentapeptide of elastin and the two analogues at temperatures below the inverse temperature transition. It is suggested that clathrate-like water surrounding hydrophobic side chains contributes to the high-frequency relaxation.

Introduction

Fibrous elastin from aorta occurs at 5–6-μm diameter fibers.[1] These fibers are comprised of a single protein, which as the soluble precursor is called tropoelastin.[2,3] A key development in deriving the molecular mechanism of biological elasticity was the finding by Sandberg and colleagues of repeating peptide sequences. The most striking repeating sequence is the polypentapeptide $(Val^1\text{-}Pro^2\text{-}Gly^3\text{-}Val^4\text{-}Gly^5)_n$, where n is 11 or greater.[4] It has been demonstrated that this polypentapeptide of elastin, also referred to as $(VPGVG)_n$ or PPP, on increasing the temperature in water undergoes an inverse temperature transition with the proposed development of a dynamic β-spiral conformation within which occurs a $Val^4\text{-}Gly^5\text{-}Val^1$ suspended segment capable of large-amplitude, low-frequency rocking motions (for a review see ref 5). The repeating pentamer in an unrolled perspective of the β-spiral is given in Figure 1.

Previous relaxation studies on the polypentapeptide of elastin[6] and on α-elastin,[7] a 70000-D chemical fragmentation product from elastin,[8] have demonstrated a single Debye-type relaxation with a relaxation time of about 7 ns at 40 °C for the polypentapeptide and about 8 ns at 40 °C for α-elastin. This relaxation has been attributed to the internal dynamics of the polypentapeptide, primarily arising from the rocking motion of peptide moieties in the suspended segment $Val^4\text{-}Gly^5\text{-}Val^1$.[6,9]

Below the temperature of the transition for the polypentapeptide, which is centered at 31 °C and begins at 24 °C, the polypentapeptide of elastin is soluble in water in all proportions. Above the temperature of the transition at concentrations less than 37% peptide by weight, two phases are observed. One is due to the more dense, viscoelastic coacervate state of the polypentapeptide, and the other is due to the transparent equilibrium solution. The polypentapeptide coacervate is a two-component system which contains by weight 63% water and 37% polypentapeptide at 30 °C.[10]

Dielectric measurements have been proven to be useful for studying water in protein. A sound discussion of this method is found in several books.[11,12] Recently, the hydration of lipoprotein,[13] protein,[14] ocular tissue,[15] brain tissue,[16,17] hemoglobin,[18] polyadenine,[19] and Na–DNA gels[20]) has been studied by dielectric relaxation measurements. (For earlier work, see ref 11 and 12.) One of the challenges of dielectric measurements is to determine

(1) Gotte, L.; Manni, M.; Pezzin, G. *Connect. Tissue Res.* **1972**, *1*, 61–67.
(2) Smith, D. W.; Weissman, N.; Carnes, W. H. *Biochem. Biophys. Res. Commun.* **1968**, *31*, 309–315.
(3) Sandberg, L. B.; Weissman, N.; Smith, D. W. *Biochemistry* **1969**, *88* 2940–2945.
(4) Sandberg, L. B.; Soskel, N. T.; Leslie, J. B. *N. Engl. J. Med.* **1981**, *304*, 566.
(5) Urry, D. W. *J. Protein Chem.* **1984**, *3*, 403.
(6) Henze, R.; Urry, D. W. *J. Am. Chem. Soc.* **1985**, *107*, 2991–2993.
(7) Urry, D. W.; Henze, R.; Redington, P.; Long, M. M.; Prasad, K. U. *Biochem. Biophys. Res. Commun.* **1985**, *128*, 1000–1006.
(8) Partridge, S. M.; Davis, H. F.; Adair, G. S. *Biochem. J.* **1955**, *61*, 11.
(9) Venkatachalam, C. M.; Urry, D. W. *Int. J. Quantum Chem., Quantum Biol. Symp.* **1986**, *12*, 15–24.
(10) Urry, D. W.; Trapnae, T. L.; Prasad, K. U. *Biopolymers* **1985**, *24*, 2345.
(11) Hasted, J. B. *Aqueous Dielectrics*; Chapman and Hall: London, 1973.
(12) Pethig, R. *Dielectric and Electronic Properties of Bilogical Materials*; Wiley: New York, 1978.
(13) Essex, G. C.; Grant, E. H.; Sheppard, R. J.; South, G. P.; Symonds, M. S.; Mills, G. L.; Slack, J. *Ann. N. Y. Acad. Sci.* **1977**, *303*, 142–153.
(14) Rejou-Michel, A.; Hencry, F.; de Villardi, M.; Delmolte, M. *Phys. Med. Biol.* **1985**, *30*(8), 831–837.
(15) Gabriel, C.; Sheppard, R. J.; Grant, E. H. *Phys. Med. Biol.* **1983**, *28*(1), 43–49.
(16) Nitingale, N. R.; Goodridge, V. O.; Sheppard, R. J.; Christie, J. L. *Phys. Med. Biol.* **1983**, *28*(8), 897–903.
(17) Steel, M. C.; Sheppard, R. J. *Phys. Med. Biol.* **1985**, *30*(7), 621–630.
(18) Schwan, H. P. *Blut* **1983**, *46*, 185–197.
(19) Takashima, S.; Casleggio, A.; Giuliano, F.; Morando, M.; Arrigo, P.; Ridella, S. *Biophys. J.* **1986**, *498* 1003–1008.
(20) Bonincontro, A.; DiBiaso, A.; Pedone, F. *Biopolymers* **1986**, *25*, 241–247.
(21) Grigera, J. R.; Mascarenhas, S. *Studia Biophysica* **1978**, *73*, 19–24.

0022-3654/88/2092-0511$01.50/0

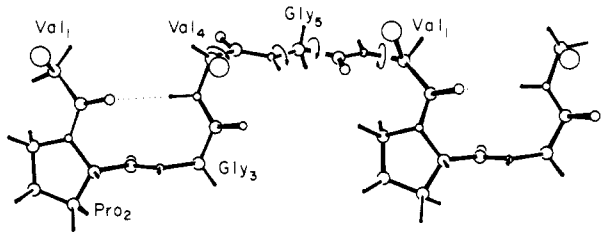

Figure 1. Unrolled perspective of the molecular structure of the β-spiral of the polypentapeptide of elastin. Reproduced with permission from *Ultrastruct. Pathol.* **1985**, *4*, 227–251.

the contributions to the so-called δ dispersion, which occurs in the range 0.1–3 GHz. This relaxation could be due to rocking motions of polar side chains or to reorientation of protein-bound water molecules. Of particular interest are the different kinds of water which could contribute in different ways to the dielectric properties and to the δ dispersion.[18] In a water–protein system, possible kinds of water would be water hydrogen bonded to dipolar and to charged groups in protein, bulk water, and (as discussed below) clathrate-like water surrounding hydrophobic side chains of the protein.

In order to examine further the rocking motion of the polypentapeptide moieties and the interaction of water within the polypentapeptide in relation to the inverse temperature transition, we have determined for comparison with PPP the dielectric properties over a frequency range 1 MHz to 1 GHz and a temperature range 0–60 °C of the two polypentapeptides: $(Leu^1\text{-}Pro^2\text{-}Gly^3\text{-}Val^4\text{-}Gly^5)_n$ and $(Ile^1\text{-}Pro^2\text{-}Gly^3\text{-}Val^4\text{-}Gly^5)_n$, also referred to as $(LPGVG)_n$ or Leu^1-PPP and $(IPGVG)_n$ or Ile^1-PPP, respectively.

Methods

Preparation of the Polypentapeptides. The preparation of Ile^1-PPP was reported earlier.[22] The synthesis of Leu^1-PPP was carried out by the classical solution methods. The polymer $(LPGVG)_n$ was synthesized by using the two monomer permutations LPGVG and GVGLP. As reported previously,[23] the sequence with Pro as the C-terminal amino acid for activation gave a higher molecular weight polymer, and the details of the synthesis of this approach (Scheme I of ref 23) will be discussed here.

As an overview, Boc-GVG-OH (III), prepared by the mixed anhydride (MA) method, was coupled with H-LP-OBzl (II) also prepared by the MA method.[24] In order to suppress the urethane byproduct formation, 1-hydroxybenzotriazole (HOBt) was added during the MA reaction.[25] Boc-GVGLP-OBzl (IV) was hydrogenated to the free acid (V) and was converted to *p*-nitrophenyl ester (ONp) by using bis(*p*-nitrophenyl) carbonate.[26] After the Boc group was removed, the peptide–ONp was polymerized in dimethyl sulfoxide (DMSO) in the presence of *N*-methylmorpholine (NMM) for 20 days. The polypeptide was taken into water and dialyzed against water by using 50-kD molecular weight cutoff dialysis tubing and lyophilized. The purity of the intermediate and final products was checked by carbon-13 nuclear magnetic resonance spectroscopy, thin-layer chromatography (TLC), and elemental analysis.

Elemental analyses were carried out by Mic Anal, Tucson, AZ. Melting points were determined with a Thomas Hoover melting point apparatus and are uncorrected. TLC was performed on silica gel plates obtained from Whatman Inc., Clifton, NJ, with the following solvent systems: (R_f^1) ethyl acetate/acetic acid/ethanol (90:10:10); (R_f^2) chloroform/methanol/acetic acid (95:5:3); (R_f^3) chloroform/methanol (5:1); (R_f^4) chloroform/methanol/acetic acid (85:15:3). Boc amino acids were purchased from Bachem Inc., Torrance, CA. HOBt was obtained from Aldrich Chemical Co., Milwaukee, WI. 1-(3-(Dimethylamino)propyl)-3-ethylcarbodiimide (EDCI) was obtained from Sigma Chemical Co., St. Louis, MO. All amino acids are of L configuration except for glycine.

Boc-Leu-Pro-Obzl (I). Boc-Leu-OH (18.69 g, 75 mmol) in dimethylformamide (DMF; 75 mL) was cooled to 0 °C, and NMM (8.25 mL) was added. The solution was further cooled to −15 °C, isobutyl chloroformate (IBCF) (9.72 mL) was added drop by drop while the temperature was maintained, and the mixture was stirred for 10 min at which time HOBt (11.48 g, 75 mmol) was added and the stirring continued for 10 min more. A precooled solution of HCl-H-Pro-OBzl (18.12 g) in DMF (65 mL) and NMM (8.25 mL) was added to the above reaction mixture. After about 20 min an additional 1 equiv of NMM was added, and the completeness of the reaction was followed by TLC. The pH of the solution was adjusted to 8 with saturated $KHCO_3$ solution, the mixture was stirred for 30 min and poured into 90% saturated NaCl solution, and the product was extracted into $CHCl_3$. After the solvent was removed, 25.5 g of I was obtained as an oil: yield 81%; R_f^1 0.96, R_f^2 0.46, R_f^3 0.95. Anal. Calcd for $C_{23}H_{34}N_2O_5$: C, 66.0; H, 8.19; N, 6.69. Found: C, 65.87; H, 8.48; N, 6.64.

Boc-Gly-Val-Gly-Leu-Pro-OBzl (IV). Boc-GVG-OH (III) (5.41 g, 16.3 mmol) and HOBt (2.75 g, 18 mmol) in DMF (50 mL) were cooled to 0 °C, EDCI (3.44 g, 18 mmol) was added, and the mixture was stirred for 20 min. To this a precooled solution of H-LP-OBzl (II) (5.8 g, 16.3 mmol), obtained by deblocking I with HCl/dioxane, and NMM (1.8 mL) in DMF (30 mL) was added, and the mixture was stirred overnight at room temperature. Solvent was removed under reduced pressure. The residue was taken in $CHCl_3$ and extracted with acid and base. After the solvent was removed the peptide was precipitated by adding EtOAc, filtered, washed with EtOAc, and dried to obtain 8.2 g of the product: yield 79%; mp 132–134 °C; R_f^1 0.75, R_f^2 0.2. Anal. Calcd for $C_{32}H_{49}N_5O_8$: C, 60.83; H, 7.82; N, 11.08. Found: C, 60.35; H, 7.97; N, 10.85.

Boc-Gly-Val-Gly-Leu-Pro-OH (V). IV (7 g, 11 mmol) in glacial acetic acid (70 mL) was hydrogenated in the presence of 10% Pd/C (0.8 g). The catalyst was filtered with the aid of Celite and solvent removed under reduced pressure. The precipitate obtained by the addition of EtOAc was filtered, washed with EtOAc and petroleum ether, and dried to give 5 g of V: yield 83.3%; mp 130–136 °C dec; R_f^3 0.2, R_f^4 0.41. Anal. Calcd for $C_{25}H_{43}N_5O_8 \cdot {}^1/_2H_2O$: C, 54.52; H, 8.05; N, 12.71. Found: C, 54.49; H, 8.38; N, 12.3.

Boc-Gly-Val-Gly-Leu-Pro-ONp (VI). V (4.5 g, 8.3 mmol) in pyridine (35 mL) was reacted with bis(*p*-nitrophenyl) carbonate (BNPC) (3.8 g, 12.46 mmol) for several days while the progress of the reaction was followed by TLC. Two additional 0.5 equiv of BNPC were added during that time. After pyridine was removed, the peptide was precipitated by added ether. VI was filtered, washed with ether, dilute citric acid, and water, and dried to obtain 4.25 g: yield 77.3%; mp 122–124 °C dec; R_f^2 0.21, R_f^4 0.7. Anal. Calcd for $C_{31}H_{46}N_6O_{10}$: C, 56.18; H, 6.99; N, 12.68. Found: C, 55.79; H, 7.02; N, 12.48.

H-(Gly-Val-Gly-Leu-Pro)$_n$-OH (VIII). The Boc group was removed from VI (3.5 g, 5.28 mmol) by treatment with trifluoroacetic acid (TFA, 30 mL) for 30 min. TFA was removed under reduced pressure, triturated with ether, filtered, washed with ether, and dried to give 3.5 g of VII. The TFA salt (VII) (3.5 g, 5.17 mmol) in DMSO (5.2 mL) was stirred for 20 days in the presence of NMM (0.91 mL, 8.3 mmol). The reaction mixture was diluted with water and dialyzed against water by using 50-kD cutoff dialysis tubing, changing the water daily for 15 days. The retentate was lyophilized to obtain 1.8 g of Leu^1-PPP (yield 79.3%). In order to remove any unreacted ONP groups present on different chains of polymer, VIII was treated with base, neutralized, dialyzed, and relyophilized.

Dielectric Relaxation Measurements. The dielectric relaxation studies were carried out by means of a coaxial line cell/vector

(22) Urry, D. W.; Long, M. M.; Harris, R. D.; Prasad, K. U. *Biopolymers* **1986**, *25*, 1939–1953.
(23) Urry, D. W.; Prasad, K. U. *Biocompatibility of Tissue Analogs*; Williams, D. F., Ed.; CRC: Boca Raton, FL, 1985; pp 89–116.
(24) Vaughan, J. R.; Osato, R. L. *J. Am. Chem. Soc.* **1967**, *89*, 5021.
(25) Prasad, K. U.; Iqbal, M. A.; Urry, D. W. *Int. J. Pept. Protein Res.* **1985**, *25*, 403–413.
(26) Wieland, Th.; Heinke, B.; Vogeler, J. *Justus Liebigs Ann. Chem.* **1961**, *655*, 189–194.

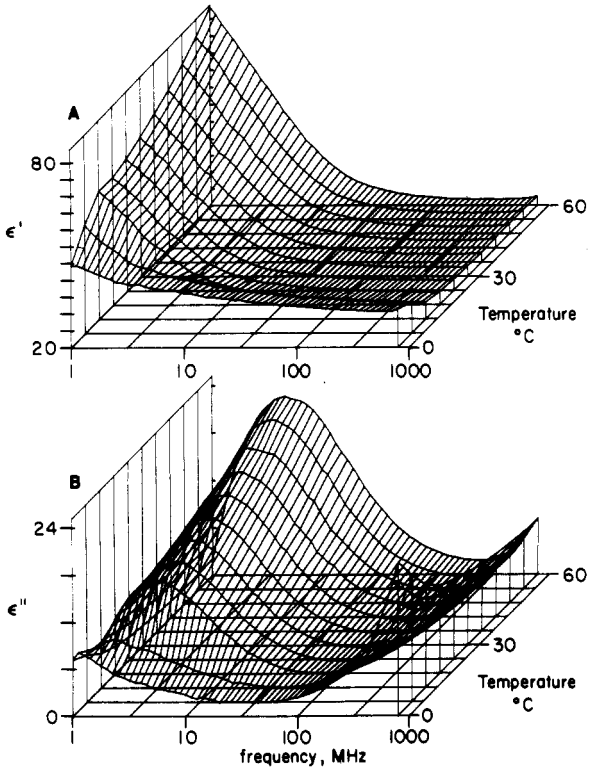

Figure 2. Real part ϵ' (A) and the imaginary part ϵ'' (B) of the dielectric permittivity of the Ile[1]-PPP over the frequency range 1–1000 MHz and over a temperature range 0–60 °C. From the imaginary part of the dielectric permittivity the conductivity term has been subtracted, which represents mainly the dielectric property of the free ions present in water. The conductivity values used are listed in Table I.

analyzer method using the Polarad Model ZPV vector analyzer with the Model E2 tuner. The signal generator used was the Wavetek Model 3510, covering the frequency range 1–1040 MHz. Both instruments were controlled by a Tektronix Model 4054 computer graphics system using an IEEE-488 Bus. The dielectric cell and the method are described elsewhere.[27,28] The temperature was controlled by a refrigerated circulating bath, Neslab Endocal RTE-5DD, and monitored by a thermocouple placed in contact with the cell using an Omega Model 410A.

The polypeptide sample was dissolved in water, coacervated at 40 °C in an injection syringe, and allowed to stand for several days at 40 °C to complete the phase separation. The coacervate concentration was carefully injected from below into the cell at a temperature below that required for the onset of coacervation where the viscosity is less. The sample was allowed to equilibrate overnight at 60 °C, a temperature above the transition temperature. Then the cell temperature was decreased to 0 °C in the period of 1 h. The cell temperature was raised in 6 °C steps from 0 to 60 °C. After each temperature was reached, the sample was allowed to equilibrate for 30 min before data collection began. The polypentapeptide of elastin, $(VPGVG)_n$ or PPP, and its two analogues, $(LPGVG)_n$ or Leu[1]-PPP and $(IPGVG)_n$ or Ile[1]-PPP, were studied.

Results

Figure 2 shows the real part (at the top) and the imaginary part (at the bottom) of the dielectric permittivity of the Ile[1]-PPP over the frequency range 1–1000 MHz and over a temperature range 0–60 °C. At each temperature, 61 logarithmic scale data points were collected for the frequency range. For the three-dimensional plots, straight line segments connected each pair of experimental data points.

Clearly, two relaxation processes can be observed. As can be seen in Figure 2, the first one is seen as an increasing relaxation process near 5 MHz when raising the temperature, and the second one shows a decreasing relaxation process within the gigahertz range when raising the temperature. Qualitatively similar results have been obtained for PPP and α-elastin.[6,7] It was suggested for PPP and α-elastin that the first relaxation is intrinsic to the polypentapeptide. More precisely, this relaxation was assigned to a peptide librational process arising primarily from the recurring suspended segment Val[4]-Gly[5]-Val[1] within the polypentapeptide. This segment, more accurately defined from the Val[4] α-carbon to the Val[1] α-carbon, is capable of low-frequency rocking motion while the other segment Val[1]-Pro[2]-Gly[3]-Val[4], from the Val[1] α-carbon to the Val[4] α-carbon, is less flexible (see Figure 1). This latter segment of polypentapeptide has a β-turn conformation involving a Val[1] C=O···H—N Val[4] hydrogen bond. The substitution of Val[1] of PPP by Ile (Ile[1]-PPP) does not modify this hydrogen bond and retains β-branching in the side chain. Thus the conformation is expected to be the same for PPP and for Ile[1]-PPP. Circular dichroism studies, in fact, show identical spectra before and after the transition.[22]

While not altering conformation, this substitution of Ile[1], however, has an important effect on the temperature of the phase transition. The phase transition temperature of the PPP coacervate is centered near 30 °C while the phase transition temperature of Ile[1]-PPP is centered near 10 °C.[22,29] As Ile is more hydrophobic than Val,[30,31] the phase transition temperature for coacervation therefore is inversely related to the hydrophobicity of the pentamer side chains.[22,29] In this perspective, the dielectric behavior of the PPP analogues provides an interesting opportunity to examine the interaction of water within these polypentapeptides. This is particularly the case because of the unusually high pentapeptide to water ratio, which provides that a greater fraction of the total water will be the unique water surrounding the hydrophobic side chains.

The second relaxation process (located within the gigahertz range) was previously attributed to water (see Figure 2). These two relaxation processes behave inversely with the temperature. Without polar side chains in the pentamers only two species, water and backbone peptide moieties, could contribute to the dielectric permittivity changes. One may wonder if other conformational states of the Ile[1]-PPP could contribute to this second process. This relaxation is observed below the phase transition, where the polymer is less ordered and the pentamers would exhibit a dispersity of conformational states with a resulting broad range of relaxation times. The polypeptide therefore is not a good candidate for the relatively intense relaxation near 1 GHz. Thus it is necessary to consider if the high-frequency relaxation process may be due to water.

In this system, at least three kinds of water are present. Free or bulk water which is not bonded to the polypeptide has a relaxation process located at 25 GHz.[11] Another kind should be water hydrogen bonded to the polar groups of the polypeptide backbone, and yet another kind, as suggested by Urry et al.[22,29] should be due to clathrate-like water associated with the hydrophobic side chains of these polypeptides which undergo inverse temperature transitions. In this regard it is now useful to consider another pentamer with yet a different hydrophobicity. Figure 3 shows the real and imaginary part of the dielectric permittivities as a function of temperature for Leu[1]-PPP. The results are very similar to Ile[1]-PPP as presented in Figure 2. Leu[1]-PPP also exhibits two relaxation processes which can be considered in the same way as previously done for Ile[1]-PPP. The phase transition for Leu[1]-PPP is centered at 15 °C, intermediate between that of Ile[1]-PPP and PPP, and the substitution of Leu instead of Val should have little effect on the Leu[1] C–O···H–N Val[4] hydrogen bond. Thus the β-spiral conformation should be the same for

(27) Henze, R.; Schreiber, U. *Ber. Bunsen-Ges. Phys. Chem.* **1984**, *88*, 1075.
(28) Göttmann, O.; Dittrich, A. *J. Phys. E* **1984**, *17*, 772.
(29) Urry, D. W.; Harris, R. D.; Long, M. M.; Prasad, K. U. *Int. J. Pept. Protein Res.* **1986**, *28*, 649–660.
(30) Nozaki, Y.; Tanford, C. *J. Biol. Chem.* **1971**, *246*, 2211–2217.
(31) Bull, H. B.; Breese, K. *Arch. Biochem. Biophys.* **1974**, *161*, 665–670.

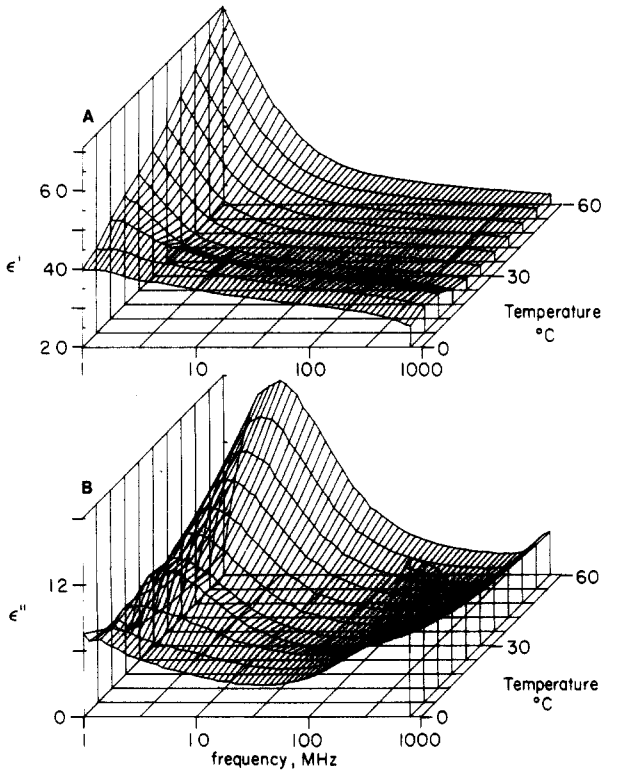

Figure 3. Real part ϵ' (A) and the imaginary part ϵ'' (B) of the dielectric permittivity of the Leu[1]-PPP over the frequency range 1–1000 MHz and over a temperature range 0–60 °C. From the imaginary part of the dielectric permittivity the conductivity term has been subtracted, which represents mainly the dielectric property of the free ions in water. The conductivity values used are listed in Table II.

Leu[1]-PPP and for PPP. The PPP results, previously reported[6] and not shown in this paper, are very similar to those of Leu[1]-PPP and Ile[1]-PPP.

A more detailed comparison of the dielectric results of the analogues shows interesting features concerning the water–polypeptide interaction which further demonstrate the origins of the near-gigahertz relaxation.

Figure 4 gives the temperature dependence of the imaginary part of the permittivity at 794 MHz for the polypeptides studied in this paper. For comparison, the temperature dependence of the permittivity (imaginary part) of pure water is shown. One can see very well the accentuated drop of the dielectric loss as a function of temperature for the polypeptides. The origin of this dielectric loss can be further considered. Free water contributes little to the dielectric loss within the polypeptide–water system at 1 GHz. It is possible that the water hydrogen bonded to the polar groups of the polypeptide backbone could give a contribution to the dielectric loss. However, another fact should be considered. Raman spectroscopy has shown that the β-turn in the polypentapeptide (with hydrogen bond) is relatively unchanged over the temperature range from 20 to 40 °C.[32] Therefore, a change in hydrogen bonding is not expected through the transition. Within the pentamer, nine polar groups are capable of hydrogen bonding (five carbonyl oxygens and four peptide hydrogens); two of these polar groups are inaccessible to water due to the intramolecular hydrogen bond of the β-turn (see Figure 1). Thus we could estimate seven sites where water molecules could hydrogen bond within the pentapeptide, but these are not expected to change significantly over the temperature range. Thus the number of polar groups hydrogen bonded to water is essentially constant. One might briefly also consider ice-like structures within the protein. However, ice has a relaxation process within the 10-kHz range,[11] and thus such highly ordered water would not contribute to the dielectric loss observed at 1 GHz.

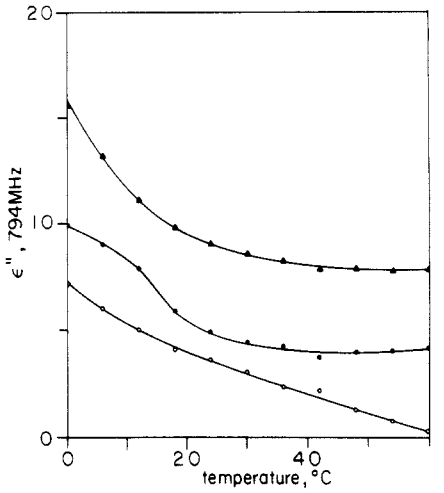

Figure 4. Temperature dependence of the imaginary part of the dielectric permittivity at 794 MHz of water (○), Leu[1]-PPP (●), and Ileu[1]-PPP (▲).

Two important facts must be noted: the first one is the high concentration of polypeptide in water (about 40%); the second one is the high content of hydrophobic groups. Thus, before the inverse temperature transition, there must be a large proportion of water associated with hydrophobic side chains. At the coacervate concentration there are approximately 30–35 water molecules per pentamer. With some 7 water molecules hydrogen bonded below the phase transition, about 25 water molecules would be either free bulk water or clathrate-like water in association with the hydrophobic side chains. It is not unreasonable that most of the 25 water molecules would be in association with the three bulky hydrophobic side chains of the pentamer of Ile[1]-PPP.

We propose that this water located in association with hydrophobic side chains of the polypeptide contributes to the dielectric loss observed at high frequency. This water should have a similar structure to water surrounding methane in clathrates,[33] and perhaps clathrate-like water therefore is an appropriate term for describing this kind of water. As all three polypentapeptides have the same number of polar groups and similar conformations, one expects that the number of water molecules hydrogen bonded to the backbone should be similar for each polypentapeptide derivative. The contribution of hydrogen-bonded water to the relaxation in the near-gigahertz range should be similar for each polypentapeptide derivative. In Figure 4, it is seen, however, that each polypentapeptide has a different magnitude of dielectric loss. It could be suggested that the number of hydrogen-bonded water molecules would not be the same for each polypentapeptide due to a restriction of access to binding sites. However, it is unlikely that Ile[1]-PPP and Leu[1]-PPP, each of which differ from PPP by a single additional CH_2 moiety, should differ from each other or even for that matter have more restricted hydrogen-bonding access than PPP. If it were a matter of steric blocking of sites, PPP would be expected to have the greater number of water molecules hydrogen bonded, and if the near-gigahertz dielectric loss were due to water molecules hydrogen bonded to the backbone, PPP should exhibit the more intense high-frequency dielectric loss. What is observed is exactly the inverse situation. Thus water hydrogen bonded to polypeptide backbone could not explain the dielectric loss. On the basis of these considerations, it is proposed that clathrate-like water contributes to the near-gigahertz dielectric loss.

Figure 5 gives the variation of the real part of permittivity at 794 Hz as a function of temperature for the polypeptides studied in this paper. Differences are apparent between the data for the polypeptides and water. While water presents a linear decrease of permittivity with increasing the temperature,[11] this is not the case for the polypeptides. A transition curve is seen. The high-frequency permittivity could reflect mainly the permittivity con-

(32) Thomas, G. T.; Prescott, B.; Urry, D. W. *Biopolymers* **1987**, *26*, 921–934.

(33) Swaminathan, S.; Harrison, S. W.; Beveridge, D. L. *J. Am. Chem. Soc.* **1978**, *100*, 5705.

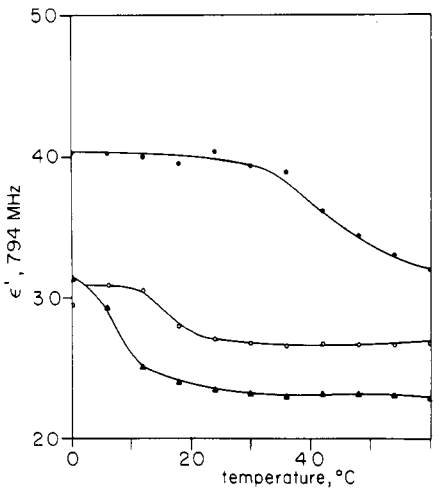

Figure 5. Real part of the permittivity ϵ' of Ileu[1]-PPP (▲), Leu[1]-PPP (○), and PPP (●) at 794 MHz as a function of the temperature.

TABLE I: Ile[1]-PPP Dielectric Relaxation Data

temp, °C	$\Delta\epsilon$	τ, ns	α	σ, mS/m	ϵ^∞ at 100 MHz ± 0.5
0[a]	26 ± 3	139 ± 6	0.36 ± 0.08	1.2 ± 0.2	32.3
6[a]	26 ± 4	87 ± 10	0.3 ± 0.1	1.8 ± 0.6	30.8
12	37 ± 2	49 ± 3	0.11 ± 0.03	0.5 ± 0.1	26.3
18	34 ± 2	44 ± 3	0.08 ± 0.02	0.6 ± 0.1	24.7
24	37 ± 3	44 ± 3	0.08 ± 0.07	0.6 ± 0.1	23.7
30	38 ± 2	38 ± 2	0.08 ± 0.02	0.6 ± 0.1	23.2
36	42 ± 3	36 ± 2	0.09 ± 0.02	0.6 ± 0.1	23
42	43 ± 3	35 ± 2	0.09 ± 0.02	0.7 ± 0.1	22.7
48	48 ± 3	39 ± 2	0.10 ± 0.02	0.7 ± 0.2	22.6
54	50 ± 3	35 ± 3	0.10 ± 0.02	0.9 ± 0.2	22.6
60	55 ± 4	31 ± 2	0.11 ± 0.03	1.0 ± 0.2	22.4

[a] The dielectric parameters of the sample at 0 and 6 °C are only suggestive since the relevant dielectric relaxation is not yet very well resolved.

TABLE II: Conductivities of Leu[1]-PPP as a Function of Temperature

temp, °C	conductivity, mS/m	temp, °C	conductivity, mS/m
0	0.3	36	1.25
6	0.27	42	1.40
12	0.57	48	1.55
18	0.67	54	1.73
24	0.96	60	1.90
30	0.9		

tribution of the water solvent. Figure 5 shows an increasing permittivity at 794 MHz from Ile[1]-PPP to Leu[1]-PPP and PPP. Thus the water content within the polypentapeptide derivative should increase from Ile[1]-PPP to Leu[1]-PPP and PPP.

Discussion

In Table I are presented the results of a curve-fitting analysis on the Ile[1]-PPP data. The dielectric permittivity was analyzed by means of one Cole–Cole function plus the conductivity term:

$$\epsilon = \epsilon^\infty + \frac{\Delta\epsilon}{1 + (i2\pi\nu\tau)^{1-\alpha}} + \frac{\sigma}{i2\pi\nu\epsilon_0}$$

where ϵ is the complex permittivity, ϵ^∞ is the high-frequency limit permittivity, $\Delta\epsilon$ is the dielectric decrement, ν is the frequency, τ is the relaxation time, α is the Cole–Cole parameter which indicates a spread of relaxation times centered about τ, σ is the conductivity, and ϵ_0 is the vacuum permittivity.

When the temperature is decreased, α of the Cole–Cole term becomes larger, indicating a spread of relaxation times which could arise from several conformational states. Above the phase transition temperature, Ile[1]-PPP develops a nearly pure Debye relaxation with α being close to zero. When the temperature is raised, the dielectric decrement becomes greater and α becomes

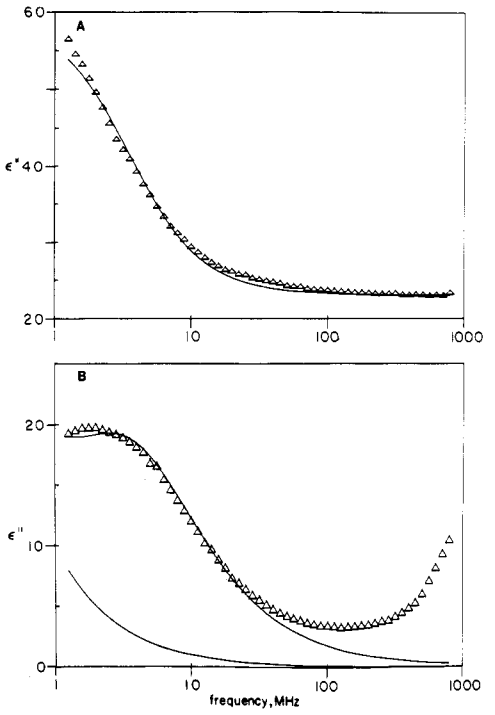

Figure 6. Example of the quality of curve fitting obtained on the Ile[1]-PPP data. The solid line represents the calculated fit, and the symbols represent experimental data. At the top (A) is the real part and at the bottom (B) the imaginary part of the dielectric permittivity of Ileu[1]-PPP at 24 °C. The other solid line curve seen at the bottom of the figure represents the conductivity.

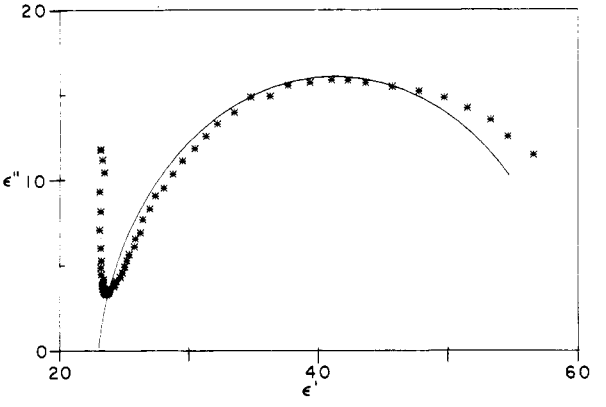

Figure 7. Cole–Cole plot of the Ile[1]-PPP sample at 24 °C. The full line is the theoretical curve, and the symbols represent the experimental data plots. The conductivity term at 24 °C (listed in Table I) has been subtracted from the dielectric loss ϵ''.

smaller, indicating an inverse temperature transition resulting in the formation of a regular structure, as can be seen qualitatively in Figures 2 and 3. As had already been reported, PPP[6] and elastin[7] develop an increasing dielectric decrement when the temperature is raised. The circular dichroism spectra of Ile[1]-PPP and PPP[22] indicate an increase of intramolecular order on raising the temperature. Thus the dielectric measurements further characterize this as an inverse temperature transition.

Figure 6 shows a typical example of the quality of curve fitting obtained on the Ile[1]-PPP data. The full line represents the best fit and the dotted points are experimental data. No attempt has been made to fit the high-frequency relaxation, since we do not know the maximum of this dielectric relaxation. The quality of the fit at low frequency (close to 1 MHz) becomes slightly less satisfactory than in the higher frequency range. Perhaps another dielectric relaxation begins to contribute at the low-frequency end of the observed range. It is also quite possible that electrode polarization would not be negligible in this frequency range. Figure 7 shows the Cole–Cole plot of the Ile[1]-PPP sample at 24 °C. At the left of the figure, the dispersion due to the clathrate-like

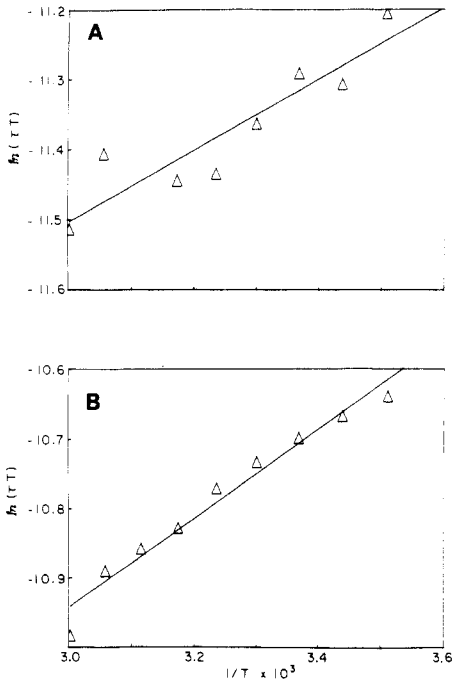

Figure 8. Temperature dependence of the correlation time (τ) from 12 to 60 °C, plotted at τT (K). The straight lines in A and B correspond to the least-squares best fit yielding an enthalpy of activation of 1.1 ± 0.2 kcal/mol (for Ile[1]-PPP in A) and of 1.3 ● 0.1 kcal/mol (for leu[1]-PPP in B). When the data point for the second highest temperature is deleted in A, the value is 1.2 ± 0.1 kcal/mol.

water is again well demonstrated.

Since the conductivity and the electrode polarization could contribute to the dielectric background, the value of the relaxation time could vary somewhat. It is still possible nonetheless to utilize the temperature dependence of the correlation time to give an estimate of the enthalpy of activation. The values from the data plotted in Figure 8 are 1.1 ± 0.2 kcal/mol for Ile[1]-PPP and 1.3 ± 0.1 kcal/mol for Leu[1]-PPP, which are similar to the value for α-elastin (1.7 kcal/mol).[7] These low energy barriers to the polypentapeptide backbone motions indicate that a dynamic structure results from the inverse temperature transition, and on γ-irradiation cross-linking the many states accessible due to the low activation energy for backbone motion provides the basis for the entropic elastomeric force exhibited by these polypentapeptide elastomers.[5,22]

Next, the high-frequency spectrum of the permittivity can be used to estimate the fractional volume of the polypeptide by means of the Maxwell–Fricke equation (usually considered appropriate for protein in solution[34-37]):

$$\frac{\epsilon - \epsilon_w}{\epsilon + x\epsilon_w} = P_i \frac{\epsilon_i - \epsilon_w}{\epsilon_i + \epsilon_w}$$

where ϵ is the measured high-frequency permittivity, ϵ_w is the high-frequency permittivity of water, ϵ_i is the high-frequency permittivity of the polypentapeptide derivative, x is the shape factor which varies between 1 and 2, and P_i is the fractional volume of the polypentapeptide derivative. For the present calculations, we chose a value of $x = 1$, which corresponds to a rigid rod shape. This choice was made because the polypentapeptide forms anisotropic fibers rather than isotropic spheres. The ϵ_i value has been computed by using the PPP data. The partial volume of PPP, which is 0.37,[10] has been used. We have found a value of ϵ_i = 5. This value has been taken for Ile[1]-PPP and Leu[1]-PPP in order to compute the partial volume. As pointed out by Dawkins,[37] a 20% uncertainty in ϵ_i results in an uncertainty of less than 4% in the calculated value P_i.

TABLE III: Comparison of the Volume Fraction of the Polypentapeptide Derivative in Water (60 °C) Computed by Means of the Maxwell–Fricke Equation[a]

	PPP	Leu[1]-PPP	Ileu[1]-PPP
volume fraction of PPP analogue	0.31 ± 0.02	0.50 ± 0.02	0.54 ± 0.03
mass fraction of PPP analogue	0.37 ± 0.02	0.57 ± 0.02	0.61 ± 0.03

[a] The errors correspond to the errors on the ϵ values only. The parameters are $X = 1$; $\epsilon_i = 5$; $\epsilon_w = 67$.

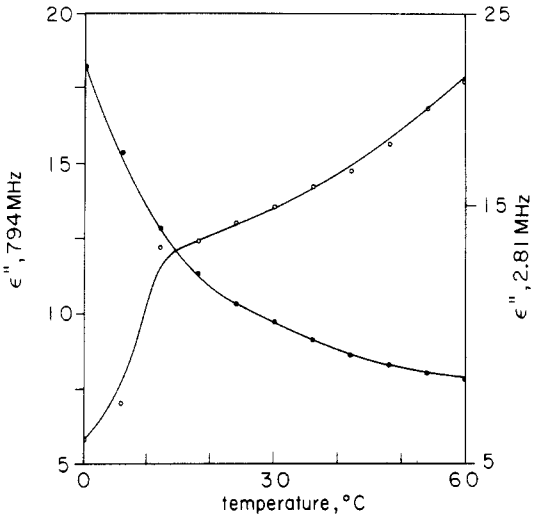

Figure 9. Imaginary part of the permittivity ϵ'' of the Ileu[1]-PPP at 794 MHz (●) and at 2.81 MHz (○) as a function of temperature. The conductivity term from the dielectric loss ϵ'' has been subtracted. The values used are listed in Table I.

The estimation of the volume fraction of the polypentapeptide derivative is presented in Table III. The water content within the polypentapeptide derivative increases in this order: Ile[1]-PPP < Leu[1]-PPP < PPP. This estimation of water content is only approximate since we do not know the exact values of the parameters. However, the data clearly demonstrate an increasing water content within the polypeptide in the order given. Interestingly, at 60 °C composition studies have shown a similar sequence for water content.[38]

Conclusions

The dielectric properties of polypentapeptide analogues of elastin in aqueous solutions provide interesting insight into the mechanism of biological elasticity and into the nature of the water within the polypentapeptide derivative.

When temperature is increased, the aqueous solutions of each polypentapeptide analogue form coacervates. By dielectric measurements a nearly simple Debye-type relaxation is observed to develop on raising the temperature, which has been attributed to peptide rocking motions of the polypentapeptide. Thus during the increase in temperature the polypentapeptide analogues become more ordered. An increase in intramolecular order on raising the temperature has also been observed by circular dichroism spectroscopy.[22]

In the high-frequency range, there is observed a dielectric relaxation which has been attributed to hydrogen-bonded water and to clathrate-like water. Since the values of the dielectric loss of PPP, Leu[1]-PPP, and Ileu[1]-PPP are not similar, water hydrogen bonded to the polypeptide backbone itself cannot explain the dielectric loss. Instead the magnitude of the dielectric loss increases with increase in hydrophobicity of the pentamer. For this reason,

(34) Pennock, B. E.; Schwan, H. P. *J. Phys. Chem.* **1969**, *73*, 2600–2610.
(35) Grant, E. H.; Sheppard, R. J.; South, G. P. *Dielectric Behavior of Biological Molecules in Solution*; Calrendon: Oxford, 1978.
(36) Jenin, P. L.; Schwan, H. P. *Biophys. J.* **1980**, *30*, 285–294.
(37) Dawkins, A. W.; Gabriel, C.; Sheppard, R. J.; Grant, E. H. *Phys. Med. Biol.* **1981**, *26*, 1–9.
(38) Waller, M.; Trapane, T.; Prasad, K. U.; Urry, D. W., unpublished data.

clathrate-like water is proposed to contribute to this high-frequency relaxation (within the gigahertz range). This high-frequency dielectric relaxation exhibits a normal phase transition, which indicates an increasing disorder on raising temperature. Thus considering the behavior of these two relaxations (one arises from the polypentapeptide backbone and the other one from the clathrate-like water or hydrogen-bonded water), there emerges an interesting picture of the temperature dependence of the water–polypentapeptide system. When the temperature is increased, the polypentapeptide derivative becomes more ordered and the clathrate-like water becomes less ordered. This inverse behavior is demonstrated in Figure 9. Thus hydrophobicity plays a role in strucutre formation in these bioelastomers, which correlates with development of elastomeric force as has been reported.[22,29]

The high frequency (1 GHz) of the dielectric permittivity of these polypentapeptide derivatives seems to correlate with the hydrophobicity of the polypentapeptide. Perhaps one of the most interesting applications of this two-component system could be the establishment of a hydrophobicity scale based on the relative amounts of observable clathrate-like water.

Acknowledgment. This work was supported in part by the Department of the Navy, Office of Naval Research Contract N00014-86-K-0402. René Buchet was supported by Swiss National Science Foundation Fellowship, and Chi-Hao Luan held a National Education Commission of the People's Republic of China Scholarship, each for a part of the research period.

Registry No. I, 83610-44-0; II, 83610-64-4; III, 96847-92-6; IV, 111583-44-9; V, 111583-45-0; VI, 111615-37-3; VII, 111583-48-3; VIII, 111583-46-1; LPGVG, homopolymer, 111583-50-7; LPGVG, SRU, 111583-51-8; IPGVG, homopolymer, 106855-57-6; IPGVG, SRU, 106855-24-7; BNPC, 5070-13-3; VPGVG, 52231-42-2; VPGVG, SRU, 111793-53-4; BOC-Leu-OH, 13139-15-6; H-Pro-OBzl·HCl, 16652-71-4.

Electrokinetic Salt Rejection by a Hypothetical One-Dimensional Inhomogeneous Charged Membrane

Scott A. Kuehl* and Ronald D. Sanderson

Institute for Polymer Science, University of Stellenbosch, Stellenbosch, South Africa *(Received: May 19, 1987)*

Rejection of ionic salt by a hypothetical one-dimensional charged-gel membrane operating in a reverse osmosis configuration is evaluated by means of different empirical forms for the spatial charge distribution. The charge density is specified while the resulting electrical potential is determined by means of a model that represents an inhomogeneous and continuous mass density of variable wavelength. The three usual sets of coupled partial differential equations that describe a convective transport process, namely, the Navier–Stokes flow, Nernst–Planck flux, and Poisson–Boltzmann equations, reduce to only two simultaneous differential equations when the flow is treated according to Darcy's law with a Debye–Bueche permeability at the high-pressure limit. Without restricting the problem to low potentials, the exact Poisson–Boltzmann equation containing the source term representing the fixed space charge is solved numerically simultaneously with an ion flux equation derived from a zero net current condition. The membrane performance for different density profiles is evaluated and discussed.

Introduction

Two approaches have been used in the theoretical modeling of solvent flow and selective ion transport through charged membranes in osmosis and reverse osmosis (RO) processes. One of these treats the membrane statically as a continuous homogeneous ion-exchange body in which it is assumed that solute rejection follows a Donnan[1-6] equilibrium (electroneutrality) at both surfaces rather than a dynamic or convective transport process throughout. Although it is expected that an electroneutrality condition should exist at both surfaces where the total charge density must reverse sign, it is not clear that a state of electroneutrality should exist everywhere else, even in a homogeneous body, nor is it obvious that membrane potential gradient should be a constant, derived from the simple Donnan potentials at the feed and permeate sides. The alternative approach is the capillary-tube model,[6-17] which correctly incorporates the dynamic coupling between the ion distribution, potential field, and hydrodynamic flow. This approach in particular is motivated in part by the simplifying advantages developed on applying the fundamental set of differential equations that describe the process, namely, the Nernst–Planck flux, Navier–Stokes flow, and the Poisson–Boltzmann equations. Other advantages of the above model, the various approximate schemes used to broaden the scope of the capillary model, and other aspects of the problem have been discussed in the literature.[6-17]

The capillary-tube hypothesis approaches its objective when it is applied to two-phase porous solids, such as compacted clays and porous glasses. These solids consist of continuous networks of insoluble or hydrophobic regions of zero permeability that form the boundaries of definite channels, the unobstructed flow of solvent through which can be adequately described by the Navier–Stokes equation. In this model the tortuous pathways and

(1) Teorell, T. *Prog. Biophys.* **1953**, *3*, 305.
(2) Glueckauf, E.; Watts, R. E. *Proc. R. Soc. London A* **1962**, *268*, 339.
(3) Glueckauf, E. *Proc. R. Soc. London A* **1962**, *268*, 350.
(4) Spencer, H. G. *Desalination* **1984**, *52*, 1.
(5) Hoffer, E.; Kedem, O. *Desalination* **1967**, *2*, 25.
(6) Dresner, L.; Johnson, J. S. *Principles of Desalination*; 2nd ed.; Spiegler, K. S.; Laird, A. D. K., Eds.; Academic: New York, 1980; Part B, Chapter 8.
(7) Dresner, L.; Kraus, K. A. *J. Phys. Chem.* **1963**, *67*, 990.
(8) Dresner, L. *J. Phys. Chem.* **1963**, *67*, 1635.
(9) Morrison, F. A.; Osterle, J. F. *J. Chem. Phys.* **1965**, *43*, 2111.
(10) Gross, R. J.; Osterle, J. F. *J. Chem. Phys.* **1968**, *49*, 228.
(11) Fair, J. C.; Osterle, J. F. *J. Chem. Phys.* **1971**, *54*, 3307.
(12) Jacazio, G.; Probstein, R. F.; Sonin, A. A.; Young, D. *J. Phys. Chem.* **1972**, *76*, 4015.
(13) Kobatake, Y. *J. Chem. Phys.* **1958**, *28*, 146.
(14) Kobatake, Y.; Takeguchi, N.; Toyoshima, Y.; Fujita, H. *J. Phys. Chem.* **1965**, *69*, 3981.
(15) Kobatake, Y.; Toyoshima, Y.; Takeguchi, N. *J. Phys. Chem.* **1966**, *70*, 1187.
(16) Sidhar, V. S.; Ruckenstein, E. *J. Colloid Interface Sci.* **1981**, *82*, 439; *J. Colloid Interface Sci.* **1982**, *85*, 332.
(17) Neogi, P.; Ruckenstein, E. *J. Colloid Interface Sci.* **1981**, *79*, 159.

0022-3654/88/2092-0517$01.50/0